Comparing different head MRI segmentation techniques for use in EEG source analysis

Abinash Pant [1,2,3], Jae-Hyun Cho[1], Carsten Wolters[2], Xiaoyi Jiang[3], Harald Bornfleth[1]
1 BESA GmbH, Gräfelfing, Germany
2 Institute for Biomagnetism and Biosignalanalysis, University of Münster, Germany
3 Faculty of Mathematics and Computer Science, University of Münster, Germany

I INTRODUCTION

Accurate segmentation of an individual human head and the resulting volume conductor model has been known to improve EEG and MEG source analysis[1][2]. However, comparison of some state-of-the-art segmentation techniques and their effectiveness in source analysis, namely Multi-Atlas[11] and Convolutional Neural Networks (CNN) [13] segmentation, is lacking. We present a comparison between these techniques to segment five tissue types using ground-truth (GT) data from BrainWeb[9].

II MATERIALS & METHODS

Multi-atlas segmentation pipeline

- Simulated atlas based on BrainWeb[9] dataset. Real dataset obtained from MRBrainS challenge.[10]
- T1 MRI images used with corresponding ground truth for white matter (WM), grey matter (GM), cerebrospinal fluid (CSF), bone and muscle.
- N4ITK[12] used for intensity inhomogeneity correction.
- 2 step registration, with a coarse affine transformation[3] step followed by a non-rigid registration[4].
- Top N atlases selected on the basis of their similarity with the target image (N=8).
- Simultaneous truth and performance level estimation (STAPLE)[11] used to decide on atlas consensus.
- Normalized cross-correlation used for local consensus.
- Morphological operations used to remove noise and isolated voxels from the final segmentation.

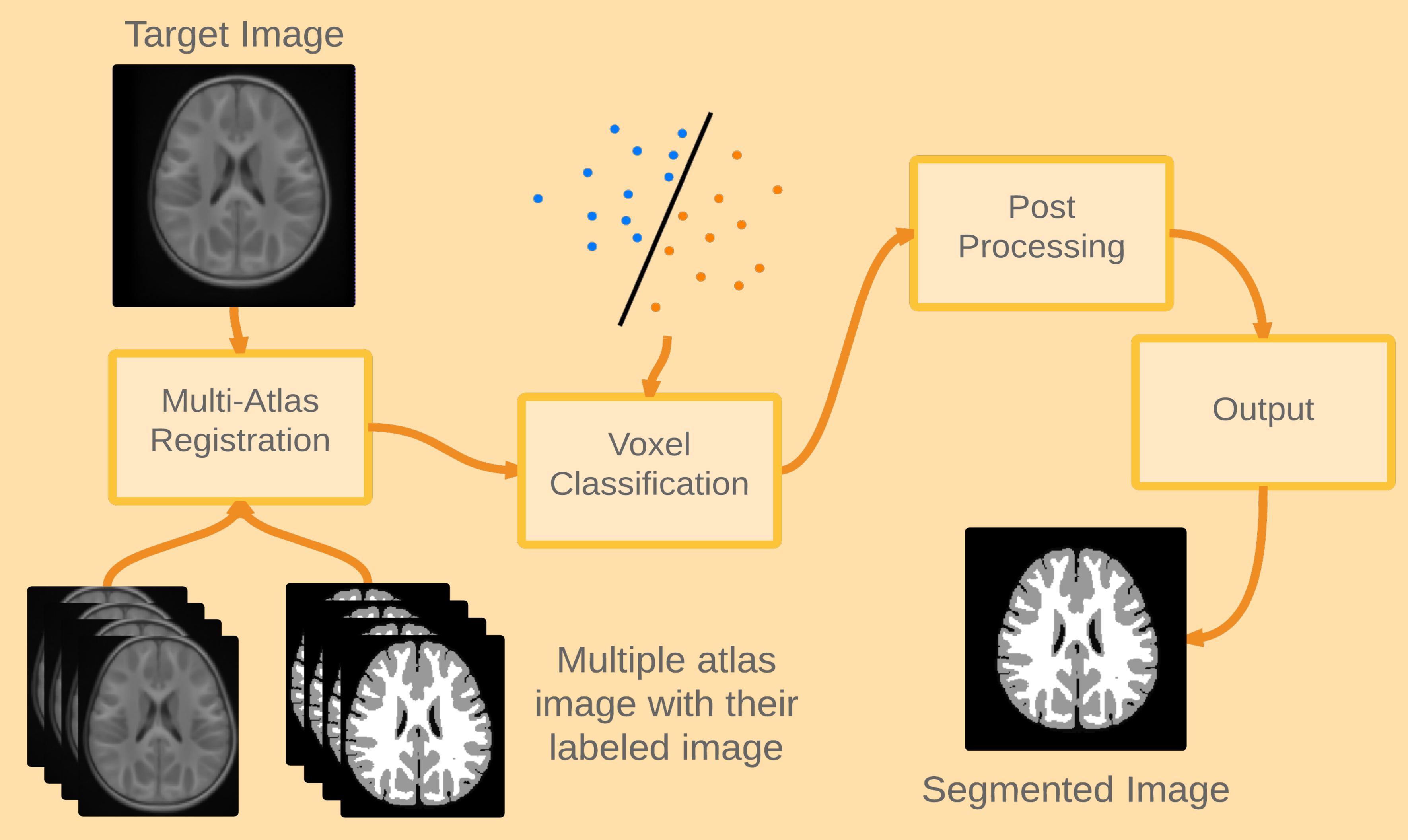

Fig. 1: Simplified multi-atlas segmentation pipeline

3D Convolutional Neural Network (3D CNN) segmentation pipeline

- 3D CNN trained to detect WM, GM, CSF, muscle and bone.
- No registration required but all images in the atlas are resampled to the same voxel size.
- Normalization of the intensity to a zero-mean, unary-variance space.
- Theano[14] framework used as the base and graphical processing unit (GPU) used for faster parallelized computation.
- Pipeline inspired by the popular multi-scale 3D CNN pipeline [13] for lesions segmentation.
- An extra pathway for a sub-sampled image is used. It is up-sampled at the classification layer.
- Final architecture 8 layers deep with a kernel of 3x3x3 voxels at every layer.
- Feature Maps of size 30, 30, 40, 40, 40, 40, 50, 50 at every layer and receptive field of size 25^3

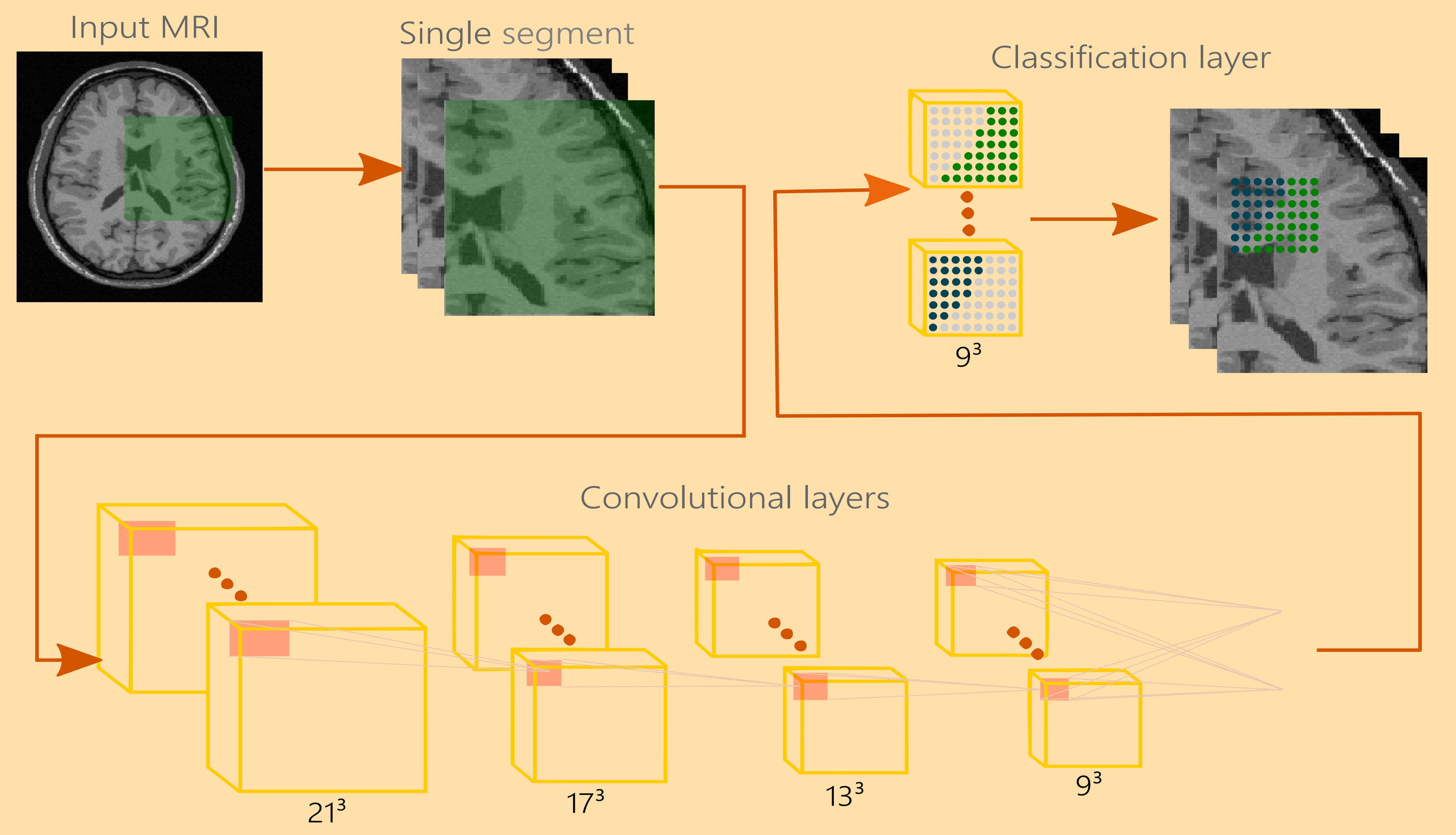

Fig. 2: An example of a simplified 4 layer deep CNN

Comparing head models of different segmentation methods

- 2000 source locations were randomly chosen inside the grey matter using a 1x1x1 mm grid.
- Each source location has 3 orientations in the 3 cardinal directions.
- Average distance between the sources was 4.13 mm.
- Simulations with 97 EEG electrodes were performed using a FEM head model.
- SimBio[15] was used to generate leadfields for ground truth data and the 2 segmention approaches.
- Magnification factor (MAG) and Relative distance measurement (RDM) values were calculated for the two segmentation techniques against the ground truth.

III RESULTS

- Three algorithms, namely STAPLE, local consensus using localized normalized cross correlation (LNCC), and 3D CNN were tested.
- For validation, 5 images were randomly selected as test images.
- Top 8 Atlases were chosen for STAPLE and LNCC using normalized mutual information (NMI).
- LNCC parameters for classifier and kernel size were tuned using 3 training images.
- Dice score was used to measure the efficacy of the 3 algorithms to detect 5 tissue classes (WM, GM, CSF, muscle and bone).

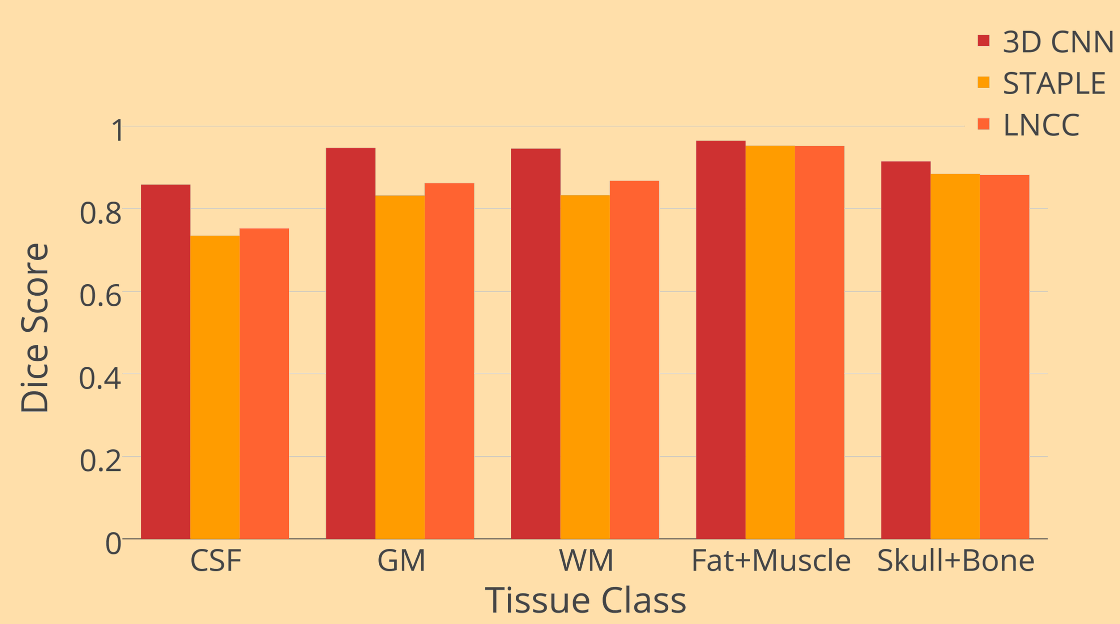

Fig. 4: A graph comparing Dice scores of 3 techniques for 5 tissue classes

Fig. 5: Output of Multi-Atlas, Ground Truth and 3D CNN

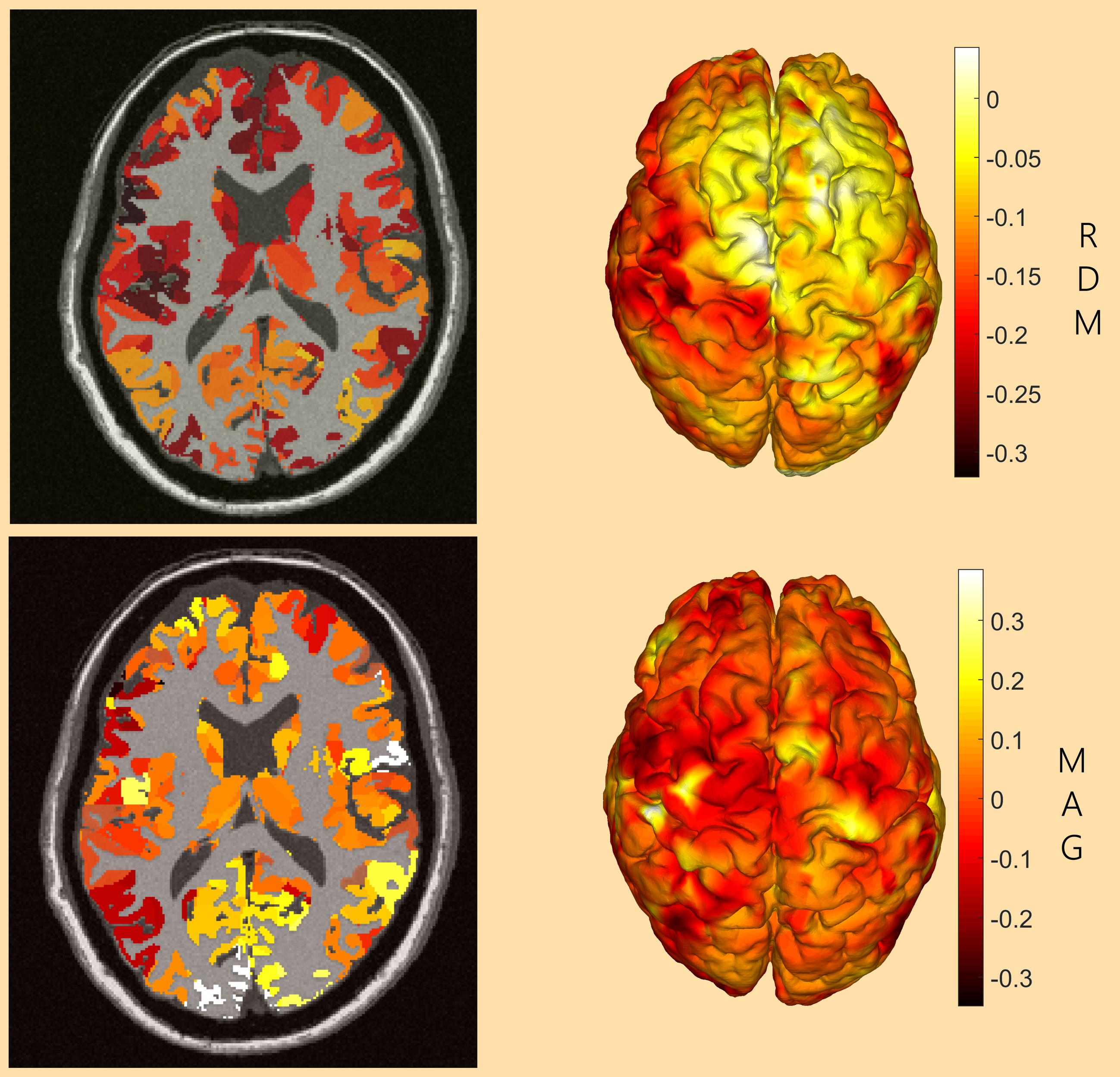

Fig. 6: Difference of RDM (top) and MAG (bottom) between CNN and MA visualised on the cortical surface (right) and volume (left)

- Mean values of the RDM and MAG for computing lead-field matrices were 0.0857, 0.9828 and 0.2051, 0.9492 for CNN and multi-atlas respectively.
- Surface and volume visualization of differnce of MAG and RDM values between CNN and MA shows CNN values being closer to the ground truth data.

IV CONCLUSIONS

The comparison of the segmentation techniques shows that 3D CNN outperforms multi-atlas based methods, especially in segmenting WM, GM and CSF. This can be attributed to the structural variability of these three tissue classes across subjects which makes it a challenging problem for segmentation algorithms based on atlas consensus, such as the multi-atlas technique. The CNN's lead-field matrix values were closest to those of the ground-truth which is in accordance with the segmentation results. The effect on source analysis will be investigated further.

[1] Yvert, B., et al. "A systematic evaluation of the spherical model accuracy in EEG dipole localization." Electroencephalography and clinical neurophysiology 102.5 (1997): 452-459.
[2] Stenroos, Matti, Alexander Hunold, and Jens Haueisen. "Comparison of three-shell and simplified volume conductor models in magnetoencephalography." Neuroimage 94 (2014): 337-348.
[3] Ourselin, Sébastien, et al. "Reconstructing a 3D structure from serial histological sections." Image and vision computing 19.1 (2001): 25-31.
[4] Modat, Marc, et al. "Fast free-form deformation using graphics processing units." Computer methods and programs in biomedicine 98.3 (2010): 278-284.
[5] Rivest-Hénault, David, et al. "Robust inverse-consistent affine CT–MR registration in MRI-assisted and MRI-alone prostate radiation therapy." Medical image analysis 23.1 (2015): 56-69.
[6] National Institutes of Health. "Retrospective Image Registration Evaluation." Vanderbilt University, Nashville (TN), USA (2003).
[7] Shi, Feng, et al. "Infant brain atlases from neonates to 1-and 2-year-olds." PloS one 6.4 (2011): e18746.
[8] SimBio Consortium. "SimBio: A generic environment for bio-numerical simulation." (2000).
[9] Cocosco, Chris A., et al. "Brainweb: Online interface to a 3D MRI simulated brain database." NeuroImage. 1997.
[10] Mendrik, Adriënne M., et al. "MRBrainS Challenge: Online evaluation framework for brain image segmentation in 3T MRI scans." Computational intelligence and neuroscience (2015).
[11] Warfield, Simon K., Kelly H. Zou, and William M. Wells. "Simultaneous truth and performance level estimation (STAPLE): an algorithm for the validation of image segmentation." IEEE transactions on medical imaging 23.7 (2004): 903-921.
[12] Tustison, Nicholas J., et al. "N4ITK: improved N3 bias correction." IEEE transactions on medical imaging 29.6 (2010): 1310-1320.
[13] Kamnitsas, Konstantinos, et al. "Efficient Multi-Scale 3D CNN with Fully Connected CRF for Accurate Brain Lesion Segmentation." arXiv preprint arXiv:1603.05959 (2016).
[14] Team, The Theano Development, et al. "Theano: A Python framework for fast computation of mathematical expressions." arXiv preprint arXiv:1605.02688 (2016).

Corresponding author:
Abinash Pant (apant@besa.de)